Hittite Journal of Science and Engineering, 2018, 5 (Special Issue: Selected Papers from ULIBTK'17) 33-49
ISSN NUMBER: 2148-4171
DOI: 10.17350/HJSE19030000117

Tree Shaped in Channels Parallel and Counter Flow Through Heat Exchanger Heat Transfer and Flow Investigation of Characteristic

A. Bugra COLAK, Isak KOTCIOGLU Mansour NASIRI KHALAJI
Ataturk University, Department of Mechanical Engineering , Erzurum, TURKEY

ABSTRACT

In this study, a heat exchanger system capable of working on tree-shaped three-level parallel and counter flow basis was designed and manufactured based on the branched Fractal like flow channel structure. A similar phylum of heat exchanger on discs onto one surface of the lower and upper plates and both surfaces of middle plate, 156 Branched-micro channels with cylindrical sections were opened in three levels symmetrically with each other at different levels and diameters. According to the parallel and counter flow type based open circuit and closed circuit principle, the fluid enters the system at equal thermal capacity ratios from the axial or radial connection points and discharges. In the open circuit operating conditions, the heating water is in the temperature range of 35-45°C and the flow rate is 2,0-4,0 lt / min. Similarly, in the closed circuit operating conditions, the heating water is in temperature range of 45-60°C and the flow rate is 2,0-4,0 lt/ min. During the experimental work, the temperature and hydrodynamic characteristics of the system are controlled through software written in the MATLAB R2013b package program. Experimental and numerical analyzes were carried out using ANSYS-Fluent ready packet programs. In the analysis, in the increasing flow rate, positions of some external and lateral channels are determined as cause of the decreasing in level of velocity. The result, requirement of designation as the bifurcation geometry divides the mass flow rate equally for each level of branching, is obtained. The results show that increase in level of branches is not important on the fluid channels which includes this kind (fractal) branch channel with tree-shaped. The results also show that, in the branched model heat exchanger, for opened and closed circuits, parallel flow (increasing branching levels, heating unit and cooling unit) is more efficient than the counter flow (increasing branching levels heating unit and decreasing branching level cooling unit) conditions.

Article History:
Received: 2018/02/28
Accepted: 2018/02/28
Online: 2018/09/07

***Correspondence to**: A. Bugra Colak, ATATURK University, Faculty of Engineering, Department of Mechanical Engineering, Erzurum, TURKEY*

Keywords:
Fractal Theory; Constructal Theory; MATLAB; ANSYS; Tree-Shaped Heat Exchanger; Parallel and Counter Flow; Branching Micro-Channel

INTRODUCTION

The cooling problem faced during use of electronic systems of industrial applications, which are designed in small size with high-performance and require high-technology, has gradually increased up to today.

Especially micro-channel heat sinks with high heat flux and an expanded surface, having an effective cooling mechanism, have gained importance. General characteristic of such heat sinks is to maximize the ability of heat rejection by minimizing volume and mass of the expanded surfaces. For higher heat transfer coefficients and minimum volume, a large surface area per unit volume provides an advantage in such channel geometries. The literature has various studies on thermal and hydrodynamic behaviours of micro-channels used as a cooling system.

A great number of scientific studies on micro-channel heat sinks have been carried out by researchers such as Tuckerman and Pease (1981), Vafai and Lu (1999), Peterson (1999), Stief et al. (1999), Chong et al. (2002), Lee et al. (2008), Moreno et al. (2015), Yang et al. (2014), Hernando et al. (2009), Bier et al. (1993). These researchers carried out thermal and flow analyses with heat exchangers designed in different geometries and with different flows in their studies. They examined optimization of single and double layered counter-flow micro-channel heat sink, and attempted to determine the optimum design parameters by carrying out thermal performance and temperature distribution analyses for micro-channel types that they have designed.

FRACTAL AND CONSTRUCTAL THEORY

In the cooling technology, the systems called *fractal channel network*, which is a symmetrical geometric structure that appears similar to itself at an infinitely little ratio and has major physical and mathematical characteristics of a non-uniform and fractured flow environment at the largest and smallest scale, have gained importance in theoretical and experimental studies in terms of applied engineering.

Fractal-like channel network is a new structure that can be assimilated to many geometric forms in the nature with its decreasing diameters from large to small. The purpose here is to obtain an appropriate surface temperature distribution without increasing the pressure drop. In the literature, the study regarding two-phase flows in the channel structures developed as similar to above mentioned structures was carried out by Daniels et al (2005).

As similar to such structures, channels known as constructal structures were also developed for the same purposes. Constructal theory is a physics law which summarizes a phenomenon existing in engineering and the nature. To express more clearly, constructal structure is a complex structure consisting of a large number of elements, and the theory defining this structure is called constructal theory. This theory is based on behaviour of various structures and forms in the nature, which are produced to obtain an optimum performance.

In the literature, most of the studies conducted on this subject are theoretical and number of experimental studies is quite low. With regard to thermodynamic optimization theory of such flow systems; researchers such as Bejan (1996, 1997, 2002, 2007), Wechsatol et al. (2002); Bonjour et al. (2003); Silva et al. (2004), Murray (1926) and Cohn (1954), Lee and Lin (1995, 1997), Lorenzini and Rocha (2006), Xia et al. (2015), Chen and Cheng (2002), Chen and Cheng (2005), Silva and Bejan (2006), Zimparov et al. (2006), Xu et al. (2006), Kwak et al. (2009), Chen et al. (2010), Heymann et al. (2010), Zhang et al. (2013), Salakij et al. (2013), Xu et al. (2015), Escher et al. (2009), Ghodoossi (2005), Andhare et al. (2016), Hong et al. (2007), Meyer et al. (2005), Kim et al. (2014), Kuen Tae Park et al. (2014) etc. developed models in their studies for estimation of pressure drops and surface temperatures in fractal-like flow channels as well as diameters and lengths of the channels. They analytically and numerically studied thermal performance of a dendritic *constructal* heat exchanger with small-scale crossflows and larger-scale counter flows.

In their studies, they compared dendritically designed fins of Y-type, T-type and H-type and numerically performed their optimal solutions that minimize their thermal resistances and increase their optimal performances. Dendritic branching-channel heat exchangers are more advantageous in terms of pressure drop when compared to other types of heat exchangers. They can also be manufactured in very small sizes, which is quite important in terms of their usability for advanced technologies such as MEMS.

In this study, a heat exchanger comprised of 3 discs with engraved branch-like cylindrical section channels was designed and manufactured, and thermal and hydrodynamic behaviours of the heat exchanger were experimentally and numerically examined by means of a test mechanism. They conducted an experimental study where pressure drop and flow energy were minimized in the test system. In addition to the experimental study; temperature, rate and pressure distributions were numerically researched through ANSYS packaged software.

MATERIALS AND METHOD

Test System

In this study, schematic drawing of the test mechanism for dendritic branching-channel heat exchanger is given in Fig. 1. The test zone of the test mechanism for the dendritic branching-channel heat exchanger is comprised of two heating units, two circulation pumps, cross flow cooling radiators, a switchboard, a computer communication unit and measuring equipment. Assembly drawing of the test mechanism equipment is shown in Figure 5. Heating and cooling sides of the dendritic branching-channel heat exchanger, which are main components of the experiment system, have been designed and manufactured to be operated with water.

Since the thermal efficiency is higher, the lower branched plate was used for heating process, while the upper branched plate was used for cooling process. The experiment system was so designed that the heating side can be

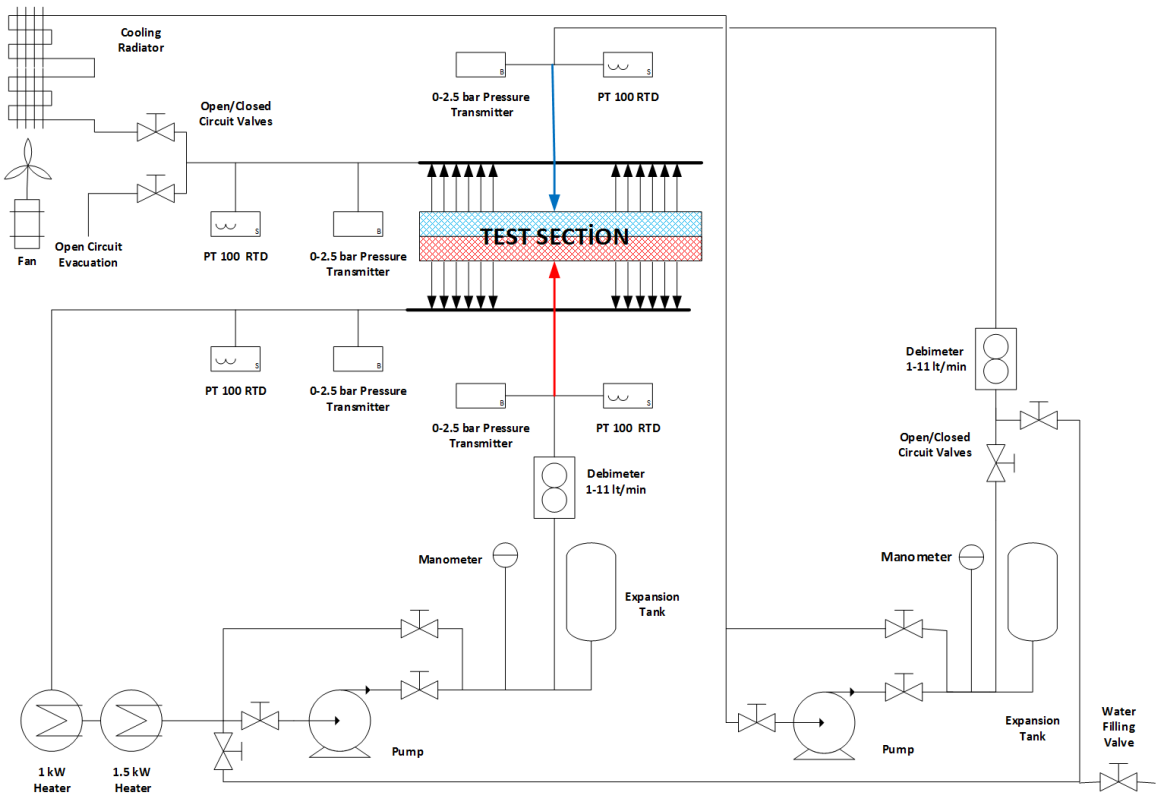

Figure 1. Schematic drawing of the test system

operated as closed circuit and the cooling side can be operated as both closed and open circuits, and tests were performed.

Schematic drawings for closed and open circuit operations are given in Fig. 2 and 3. In order to enable fluid circulation in heating and cooling units, two circulation pumps with the same power was used one for each fluid circuit.

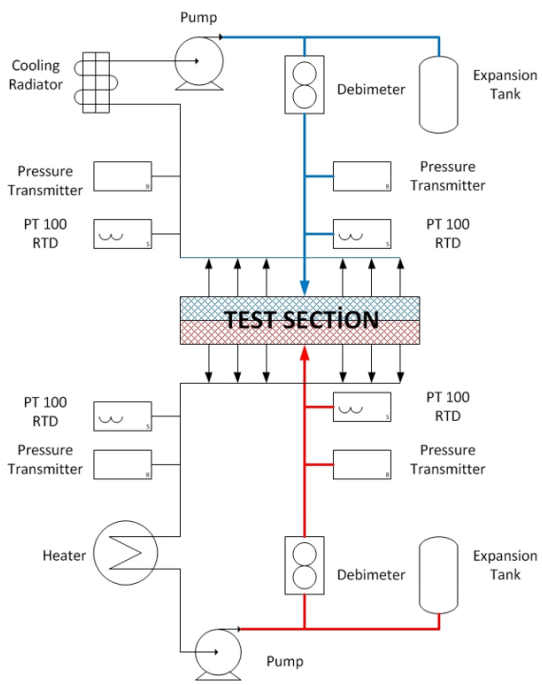

Figure 2. Closed circuit operation of the test system

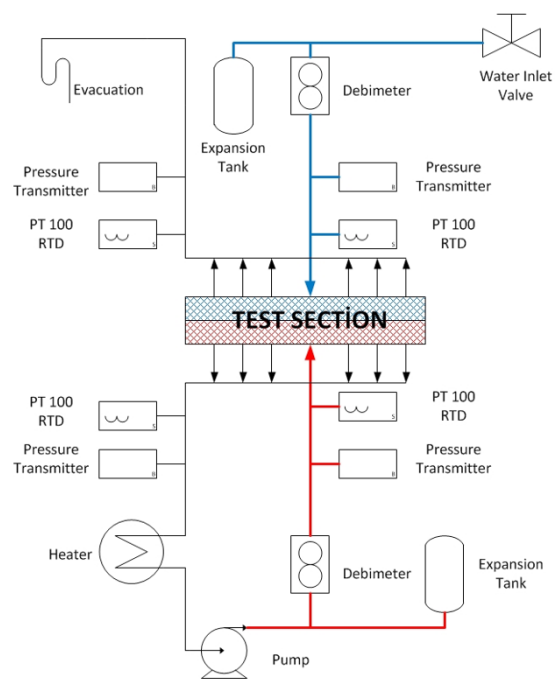

Figure 3. Open circuit operation of the test system

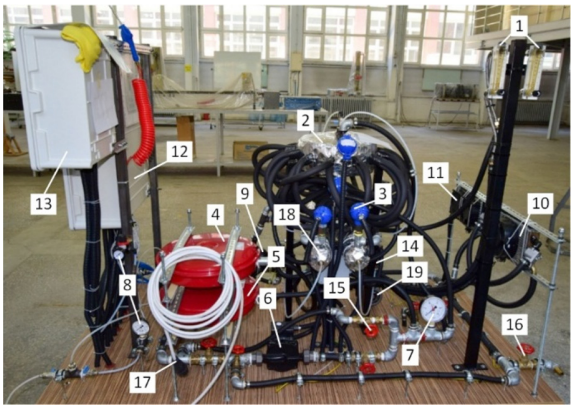

Figure 4. Components of the test system; **(1)** Flowmeter **(2)** Test Zone **(3)** PT100 Temperature Transmitter **(4)** Expansion Tank (Heating Side) **(5)**Expansion Tank (Cooling Side) **(6,19)** Circulation Pump **(7)** Hydrometer **(8)** Pressure Gauge **(9)** Heating Tank **(10)** Cooling Radiator **(11)** Cooling Fan **(12)** Switchboard **(13)** Electronic System Panel **(14)** Pressure Transmitter **(15)** Bypass Valve **(16)** Filling Valve **(17)** Power Connection **(18)** Collector

Both circuits were set with float flowmeters to measure the amount of the fluid. In addition, 2 sleeve-type resistance heaters were used in order to heat the fluid used in the heating side.

It has two electrically operated heaters, each of which is situated into an individual small-volume tank, with the power of 1 kW and 1.5 kW; and the fluid is transmitted into the system after consecutively passing through these two heaters.

The heaters were not controlled by a separate thermostat; instead, they were precisely set through MATLAB software, which allows operation of the test system and receiving the test data, and controlled through contactor groups. The experiment system was controlled and stabilized beforehand through the pre-heating software prepared in MATLAB software package, and tests were started after pre-heating process.

Heat Transfer Process

In this study, the fluid in the heating side (hot water) circulates through the test system on a closed circuit basis and the fluid in the cooling side (cold water) circulates through the system on both open circuit and closed circuit bases. Under the closed circuit operating conditions, the fluid exiting from the test zone as heated is cooled by the radiators, then pressurized by the circulation pump and returned to the test zone. Under the open circuit conditions, the fluid entering the cooling unit is taken from the mains system, and pressure of the mains is used for circulation in the system. The heated fluid exiting from the test zone leaves the system after its temperature is measured. Heat transfer values of the fluids entering into and exiting from the heating and cooling sides during the tests were individually calculated. In calculation, heat transfer values for entry and exit are averaged and the following equation is used,

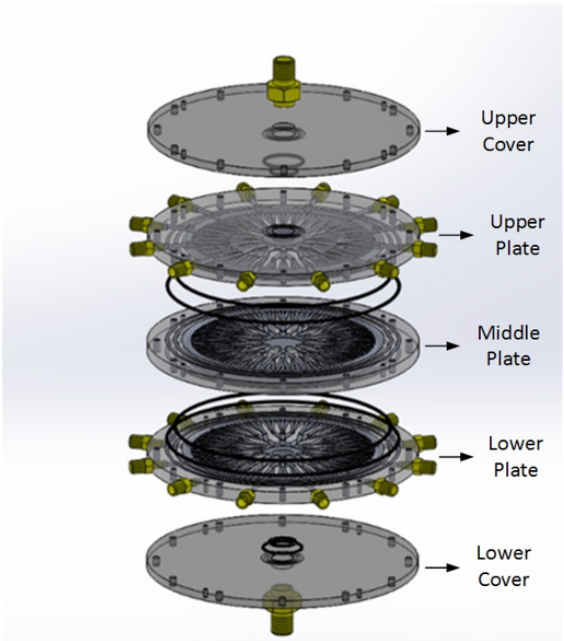

Figure 5. Test zone of the test system

$$Q_{mean} = \frac{Q_g + Q_r}{2} \quad (1)$$

In this equation, Q_g is the heat transfer value for entry into the system and Q_r is the heat transfer value for exit from the system. Heat balance of the system is given with the equation below.

$$Q_{top} = Q_{transm} + Q_{con} + Q_{rad.} + Q_{losses} \quad (2)$$

The heat loss in the test zone due to radiation is about 5% of the heat received from the fluid entering into the dendritic branching-channel heat exchanger. Since this value can be omitted when compared to the heat transfer value at the fluid inlet, and the equation is rearranged as below;

$$Q_{top} = Q_{transm} + Q_{con} + Q_{losses} \quad (3)$$

The heat transfer to the system due to the hot fluid passing through between the lower and middle plates is calculated with the following equation.

$$Q_g = \dot{m}_h C_p \left(T_1 - T_2\right) \quad (4)$$

In this equation, T_1 temperature is the inlet temperature of the hot fluid entering into the dendritic branching-channel heat exchanger. T_2 temperature is the outlet temperature of the hot fluid exiting from the collector. The heat transfer from the system due to the cold fluid passing through between the upper and middle plates is calculated with the following equation.

$$Q_r = \dot{m}_c C_p \left(T_4 - T_3\right) \quad (5)$$

In this equation, T_3 temperature is the inlet temperature of the cold fluid entering into the heat exchanger. T_4 temperature is the outlet temperature of the cold fluid exiting from the collector. Similarly, the heat loss can be calculated as below,

$$Q_{\%thermal\ difference} = \left(1 - \left(\frac{Q_r}{Q_g}\right)\right) x100 \quad (6)$$

R.S. Andhare et al. (2016) stated that this thermal difference can be at 10% level; and this ratio was calculated in our studies and given as a diagram in Fig. 17.

Reynolds (Re) Prandtl (Pr) and Nusselt (Nu) Numbers

In calculation of the flow and the heat transfer, the flow inside a cylindrical section pipe and relevant pure numbers are given with the equations below.

$$Re = \frac{\rho V D_h}{\mu} \quad (7)$$

Prandtl number, which is the ratio of momentum diffusion to thermal diffusion in the thermal and hydrodynamic boundary layers, was calculated with the following equation;

$$Pr = \frac{\nu}{\alpha} = \frac{c_p \mu}{k} \quad (8)$$

In this equation, (ν) is kinematic viscosity, (α) is thermal diffusivity, (c_p) specific heat, and (μ) is dynamic viscosity. Separate Nusselt numbers for fully developed and developing flows are given in the following equation, for a cylindrical section pipe with a diameter of D_h, according to (h) heat transfer coefficient and k heat convection coefficient.

$$Nu = \frac{hD_h}{k} \quad (9)$$

In the dendritic branching-channel heat exchanger test mechanism, thermally and hydrodynamically developing laminar flow conditions have been applied to the flow in the heat exchanger up to a flow rate of 4.0 l/min at branching level 0. Thermally and hydrodynamically developing flow conditions have been applied to all ranges of flow rate at branching levels 1 and 2.

Nusselt correlations required for this study depending on the Reynolds number, the flow regime and the thermal conditions are given below.

Branching and Branch Levels Measurement Details

Design specifics of the dendritic branching-channel heat exchanger are given in Fig. 6. In this type of heat exchangers; *N number of branching* means number of the branches to be developed by the current channel at the next level, and k branching level means the number of branching points starting from the fluid inlet. For the heat exchanger modelled in this study, N=3 and k=2, i.e. k=0, k=1, k=2. As it is seen in Figure 6, D_0, D_1 and D_2 and L_0, L_1 and L_2 indicate channel diameters and lengths for three different levels from level zero to level two, respectively. As it is shown in Fig. 8; starting from the inlet point, the fluid splits into 12 branches at level 0, and then it splits again into 3 at level 1 thus creating 36 branches. At level 3, the fluid splits into 3 again, thus creating 108 branches. The fluid arrives the collecting channel after branching level 2 and leaves the heat exchanger by passing through the 12 discharge points located there.

Table 1. Nu number correlations for developing flows (Stephan,Preusser)

Reynolds Number	*Flow Regime*	*Thermal Conditions*
Re<2300	*Thermally and Hydrodynamically Developing Flow*	*Constant heat flux*
$Nu = 4.364 + \frac{0{,}086\left(\frac{RePrD}{L}\right)^{1.33}}{1 + 0.1Pr\left(\frac{ReD}{L}\right)^{0.83}}$		
Re<2300	*Thermally and Hydrodynamically Developing Flow*	*Constant Surface Temperature*
$Nu = 3.657 + \frac{0{,}0677\left(\frac{RePrD}{L}\right)^{1.33}}{1 + 0.1Pr\left(\frac{ReD}{L}\right)^{0.3}}$		

Technical details of the plates of the dendritic branching-channel heat exchanger are given in Fig. 6, Fig. 7 and Fig. 8. On the plate, there are 12 branches at level 0, 36 branches at level 1 and 108 branches at level 2. The symmetrical branching spreading on the disc-shaped plate is produced from aluminum material according to the technical details thereof given in Table 2.

Total area of the branching spreading on the heat exchanger at level N is calculated separately for each level with the following equation.

$$A_k = \pi\, x\, N_k\, x\, D_{h,k}\, x\, L_k \quad (10)$$

$N_k = 12\left(3^k\right)$ In this equation, (N_k) is the number of the branches at level k, and , $D_{h,k}$ is hydraulic diameter of the branch at level. (L_k), is the length of the branch at level k. According to the equation 10, relevant areas at level 0, level 1

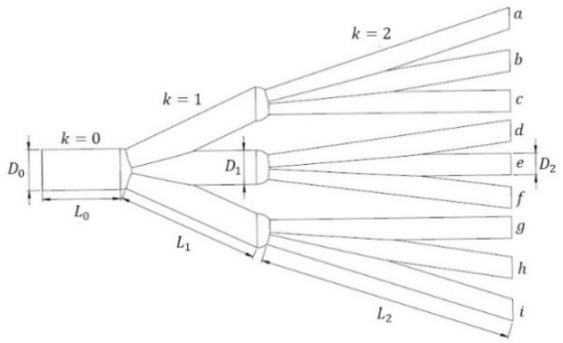

Figure 6. Branching details of the dendritic branching-channel heat exchanger

and level 2 are A_0=2,601 x $10^{(-3)}$m^2, A_1=0,0113 m^2, A_2=0,04033 m^2, respectively. Total area is calculated as $A_{top}=A_0+A_1+A_2$=0,05423 m^2.

Total Heat Transfer Coefficient (U)

Heat is transferred from resistances between fluid-wall-fluid due to $(T_h - T_c)$ temperature differences. When equal surface areas are considered, total heat transfer coefficient (U) is obtained with the following equation,

$$\frac{1}{U}=\frac{1}{h_h}+\frac{t}{k}+\frac{1}{h_c} \tag{11}$$

U is total heat transfer coefficient, $1/h$ is convection resistances, and t/k is transfer resistance. Heat transfer values were calculated separately on the basis of mass flows, inlet and outlet temperatures and thermal capacities of both fluids. Heat transfer from hot fluids is found by using the equation below,

$$Q_h=\dot{m}_h c_p\left(T_{h,i}-T_{h,o}\right) \tag{12}$$

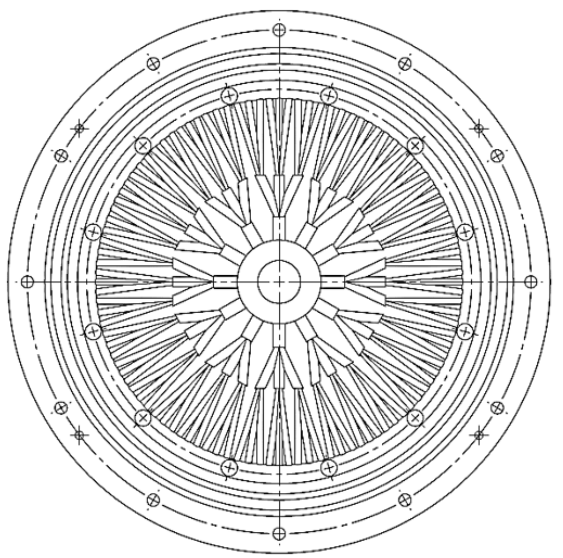

Figure 7. Upper and lower plate details of the dendritic branching-channel heat exchanger

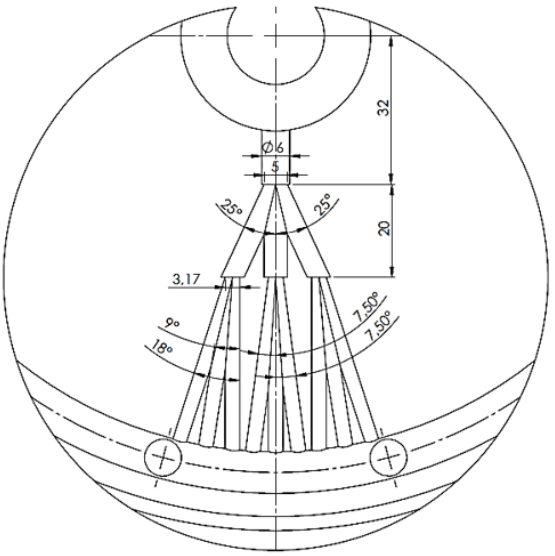

Figure 8. Technical drawing of branching details of the dendritic branching-channel heat exchanger

Similarly, heat transfer to cold fluid is calculated by using the following equation,

$$Q_c=\dot{m}_c c_p\left(T_{c,i}-T_{c,o}\right) \tag{13}$$

Coefficient for total heat transfer between the hot fluid and the inner surface of the plate is found through the equation below,

$$U=\frac{Q_h}{A_{top}\dfrac{\left(T_{h,i}-T_{c,i}\right)-\left(T_{h,o}-T_{c,o}\right)}{ln\dfrac{\left(T_{h,i}-T_{c,i}\right)}{\left(T_{h,o}-T_{c,o}\right)}}} \tag{14}$$

In these equations, Q_h is heat transfer from the hot fluid, $T_{h,i}$ is temperature of the hot fluid entering into the heating side of the heat exchanger, $T_{h,o}$ is temperature of the cooled fluid exiting from the heating side of the heat exchanger, $T_{c,i}$ is temperature of the fluid entering into the cooling side of the heat exchanger, $T_{c,o}$ is temperature of the heated fluid exiting from the cooling side of the heat exchanger, and A_{top} is total surface area of the branching spreading on the heat exchanger.

Log Mean Temperature Difference (LMTD)

In the thermal analysis of the heat exchanger, the Log Mean Temperature Difference (LMTD) method and the

Table 2. Geometric properties of the fractal channels

Branching Level	*Number of the Channels in a Branch*	*Hydraulic Diameter*	*Branch Length*
k	N_k	$D_{h,k}\,(mm)$	$L_k\,(mm)$
0	*12*	*6.00*	*11.50*
1	*36*	*5.00*	*20.00*
2	*108*	*3.17*	*37.50*

ε *-NTU* method were used. In the log mean temperature difference method, heat transfer value of the heat exchanger is calculated with the equation given below.

$$\dot{Q} = UA\Delta T_{lm} \tag{15}$$

Log mean temperature difference in the equation above is given with the following equation,

$$\Delta T_{lm} = \frac{\Delta T_1 - \Delta T_2}{\ln\left(\frac{\Delta T_1}{\Delta T_2}\right)} = \frac{\left(T_{h,i} - T_{c,i}\right) - \left(T_{h,o} - T_{c,o}\right)}{\ln\left(\frac{T_{h,i} - T_{c,i}}{T_{h,o} - T_{c,o}}\right)} \tag{16}$$

For log mean temperature difference in a parallel flow heat exchanger, ΔT_1 and ΔT_2 temperature differences at inlet and outlet points are calculated as below,

$$\Delta T_1 = T_{h,i} - T_{c,i} \quad (17) \text{ and } \quad \Delta T_2 = T_{h,o} - T_{c,o} \tag{18}$$

In these equations, $T_{h,i}$ is inlet temperature of the hot fluid entering into the heat exchanger, $T_{c,i}$ is inlet temperature of the cold fluid entering into the heat exchanger, $T_{h,o}$ is outlet temperature of the hot fluid exiting from the heat exchanger, and $T_{c,o}$ is outlet temperature of the cold fluid exiting from the heat exchanger.

For log mean temperature difference in a counter-flow heat exchanger, ΔT_1 and ΔT_2 temperature differences at inlet and outlet points are calculated as below,

$$\Delta T_1 = T_{h,i} - T_{c,o} \quad (19) \text{ and } \quad \Delta T_2 = T_{h,o} - T_{c,i} \tag{20}$$

At the same inlet and outlet temperatures of the heat exchanger, log mean temperature difference was found higher in case of counter-flow when compared to parallel flow.

ε -NTU Method

Before defining effectiveness for a heat exchanger, the maximum possible heat transfer value Q_{max} should be calculated for that heat exchanger. In such case, $(T_{h,i} - T_{c,o})$ maximum heat transfer will occur due to the maximum difference of temperature obtained between the fluids in the heat exchanger.

For this, the thermal capacity flow rate $C_c = \dot{m}_c c_p$, of the cold fluid must be lower than the thermal capacity flow rate $C_h = \dot{m}_h c_p$ of the hot fluid ($C_c < C_h$). In this case, it would be $|dT_c| > |dT_h|$. For r, $L \to \infty$, outlet temperature of the cold fluid can rise up to inlet temperature of the hot fluid where $C_c < C_h \; and \; T_{c,o} = T_{h,i}$, Q_{max} is obtained with the equation below,

$$Q_{max} = C_c\left(T_{h,i} - T_{c,i}\right) \tag{21}$$

Similarly, if $C_h < C_c$, a bigger exchange of heat would occur in the hot fluid and it can get cooled down to the inlet temperature of the cold fluid. Where $C_h < C_c$ and $T_{h,o} = T_{c,i}$, Q_{max} is given in the following equation.

$$Q_{max} = C_h\left(T_{h,i} - T_{c,i}\right) \tag{22}$$

In these two cases, Q_{max} heat transfer value is given according to the minimum heat capacity $C_{\min}$ in the equation below.

$$Q_{max} = C_{min}\left(T_{h,i} - T_{c,i}\right) \tag{23}$$

In this equation, $C_{\min}$ thermal capacity flow rate is accepted equal to the lower one of *Cc* or C_h values. In a heat exchanger, the ratio of the actual heat transfer Q value to the maximum possible heat transfer Q_{max} value is defined as ε effectiveness, and presented with the following equation.

$$\varepsilon = \frac{Q}{Q_{max}} \tag{24}$$

Effectiveness ε can also be calculated on the basis of temperature difference and thermal capacities through the equation below.

$$\varepsilon \equiv \frac{C_h\left(T_{h,i} - T_{h,o}\right)}{C_{min}\left(T_{h,i} - T_{c,i}\right)} \tag{25}$$

In this relation, $C_{\min}/C_{\max}$ ratio can take C_c/C_h or C_h/C_c value, depending on thermal capacity flow rates of the hot and cold fluids. *NTU Number of Transfer Unit* is equal to the ratio of total heat transfer coefficient and heat transfer surface area to the minimum thermal capacity, and given with the following equation.

$$NTU \equiv \frac{UA}{C_{min}} \tag{26}$$

Effectiveness-NTU Relations

$C_{\min}=C_h$ let a parallel flow heat exchanger with is considered. If the effectiveness value ε for a parallel flow heat exchanger is found;

$$\varepsilon = \frac{1 - exp\left\{-NTU\left[1 + \left(C_{min} / C_{max}\right)\right]\right\}}{1 + \left(C_{min} / C_{max}\right)} \tag{27}$$

$C_{\min}=C_c$ since the same result is obtained for; regardless of whether the minimum thermal capacity flow rate of fluid belongs to the hot fluid or the cold fluid, this relation can be applied to any parallel flow heat exchanger. When C_r<1, the effectiveness value for counterflow operating conditions is given with the equation below,

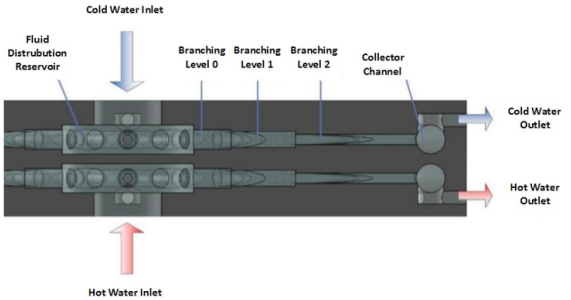

Figure 9. Sectional view of parallel flow operation of the dendritic branching-channel heat exchanger

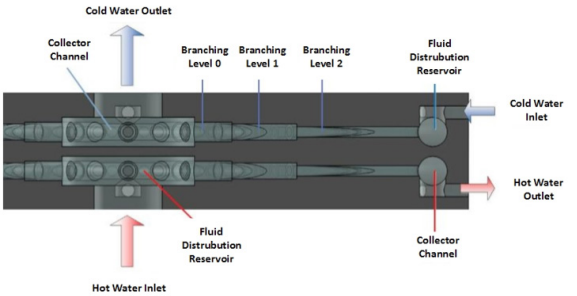

Figure 10. Sectional view of counter-flow operation of the dendritic branching-channel heat exchanger

$$\varepsilon = \frac{1 - exp\{-NTU\,(1 - C_r)\}}{1 - C_r\, exp\{-NTU\,(1 - C_r)\}} \tag{28}$$

In case that C_r=1, effectiveness value is given with the following equation,

$$\varepsilon = \frac{NTU}{1 + NTU} \tag{29}$$

In this study, tests were conducted by assuming that flow rates of both fluids are equal; and thermal capacity flow rates of both fluids are equal (C_{min}=C_{max}).

RESULTS

Thermal Transfer Analysis

In this study, while thermal capacity flow rates of the designed dendritic branching-channel heat exchanger at its upper-middle and lower-middle plates were kept equal, operation at similar fluid inlet temperatures (closed circuit) and operation at distinct fluid inlet temperatures (open circuit) were studied. Performances of parallel flow and counter-flow configurations were compared. In Fig. 9 and Fig. 10, representative sectional views of the heat exchanger in cases of parallel flow and counter-flow are given. Findings obtained from the tests conducted under operating conditions of the parallel flow closed circuit are given as a diagram in Fig. 11. In this diagram, change of the heat transfer value (Q) by the volumetric flow rate ($\dot{V}$) at different temperatures in case of the parallel flow closed circuit is presented. It is observed that the heat transfer value increases at the same ratio with each increase of temperature. For the values lower than 4 liter/minute volumetric flow rate, laminar flow conditions apply at branching levels 0, 1 and 2 of the dendritic branching-channel heat exchanger.

For the volumetric flow rate values over 4 liter/minute, it was seen in the calculations that the turbulent flow conditions applies at level 0. When the inlet water temperature ($T_{h,i}$) rises over 60°C, turbulent flow conditions occur in branches at levels 0 and 1 at a volumetric flow rate of 9,0 liter/minute.

When change of the heat transfer values and the volumetric flow rates are compared between the parallel flow closed circuit given in Fig. 11 and the counter-flow closed circuit given in Fig. 12, it is seen that the heat transfer value is higher for the parallel flow at the same volumetric flow rate. Flow conditions occurring toward increasing branching levels also increase the amount of the transferred heat while increasing pressure losses. In the computer-aided study carried out under this research, it was seen that the outlet temperature values obtained for both sides as a result of the analyses performed through ANSYS-Fluent software package were approximately equal to the outlet temperature value of the fluid exiting from the system in the tests.

In the diagrams in Fig. 13 and Fig. 14, changes of the heat transfer values of the parallel flow and counter-flow open circuits respectively by the volumetric flow rate of the fluid are separately presented. In these diagrams, it is seen that the parallel flow open circuit is more effective than the counterflow.

In the diagram in Fig. 15, the ratio of the heat transfer value to the inflowing heat value at the same temperature and flow rate values (45°C, 2.0-4.0 l/min) for the tests conducted in closed and open circuits is presented. Under the same conditions, this ratio is higher for the open circuit.

$$Q_{\%thermal\ difference} = \left(1 - \left(\frac{Q_r}{Q_g}\right)\right) x100 \tag{30}$$

Pressure Losses

In order to find the pressure losses for increasing and decreasing levels of branching of the dendritic branching-channel heat exchanger, pressure losses were measured at flow rates between 2.0-9.0 l/min. For measuring purpose, pressure transmitters situated at fluid inlet and collector outlet points of the dendritic branching-channel heat exchanger were used.

As it is seen in Fig. 16, Reynolds number in the heat exc-

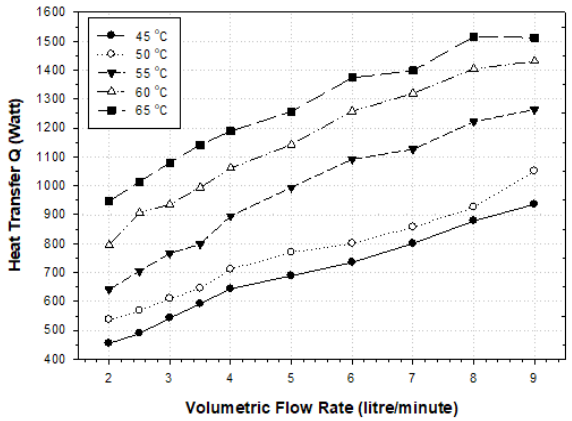

Figure 11. Change of the heat transfer value by the volumetric flow rate in the parallel flow closed circuit

hanger consisted of cylindrical section branching increased by increasing volumetric flow rate, and it caused an increase

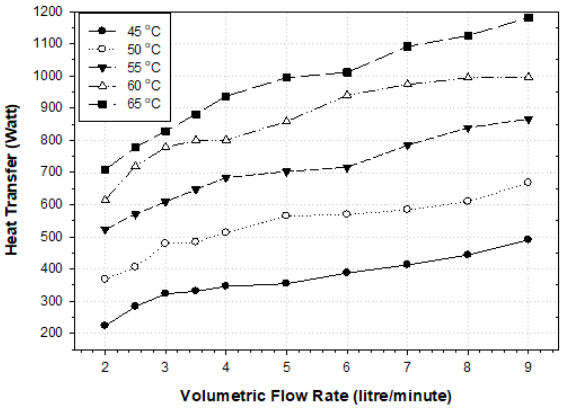

Figure 12. Change of the heat transfer value by the volumetric flow rate in the counterflow closed circuit

also in the pressure losses. The flow is laminar at the flow rates below 4.0 l/min at all branching levels. In the laminar flow region, Reynolds numbers range between 200-1950. After the volumetric flow rate of 4.0 l/min, a transition from

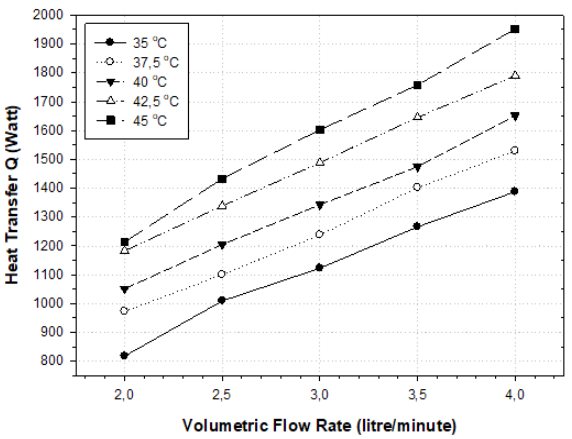

Figure 13. Change of the heat transfer value by the volumetric flow rate in the parallel flow open circuit

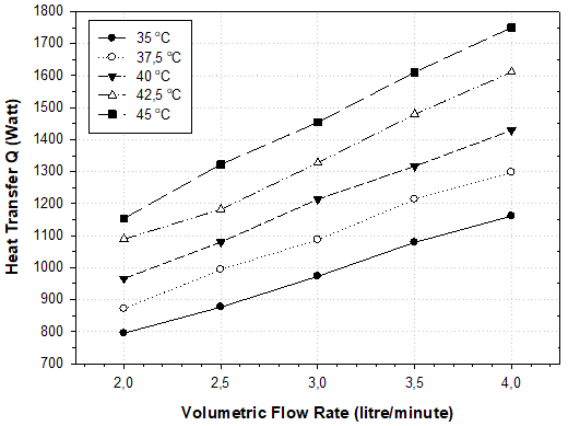

Figure 14. Change of the heat transfer value by the volumetric flow rate in the counterflow open circuit

laminar flow to transient region occurs for branching level 0.

As it is seen in the diagram, the pressure losses towards increasing branching levels are higher than those towards decreasing branching levels in case of the laminar flow. It is seen that a transient flow occurs after 4.0 l/min value at branching level 0 and the pressure and its losses are almost equal for the flows toward both ways. At other branching levels, the flow is laminar for both flow conditions. At branching levels 1 and 2, the flow rate decreased further. This result indicates that further branching is not important in the flow channels with such dendritic branching (fractal) channel structure. This situation shows that, in terms of shedding light on the limited number of studies carried out on this subject, and experimental result in this study is consistent with the theoretical and experimental results in the literature.

Log Mean Temperature Differences

In order to be able to experimentally calculate the total heat transfer coefficient (U) in a heat exchanger, the log mean temperature (ΔTLM) difference method is used. In the experiments carried out for the dendritic branching-

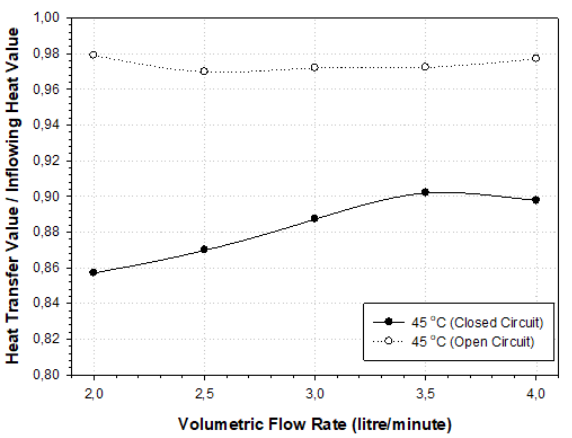

Figure 15. Change of the ratio of the heat transfer value / inflowing heat value by the volumetric flow rate in cases of closed and open circuits

channel heat exchanger, changes between the volumetric flow rates and the log mean temperature differences for different operating conditions and different situations are separately presented in the diagrams in Fig. 17-20. When Fig. 17 and Fig. 18 are compared, the log mean temperature difference is higher in the parallel flow closed circuit when compared to the counter-flow closed circuit.

Change of Nusselt-Reynolds Numbers

The change of the Nusselt numbers calculated for the heating and cooling sides at a maximum heating water inlet temperature of 65°C under the operating conditions of the parallel flow closed circuit by the Reynolds number is given in Fig. 21. According to the Nu relation given above, change of the Nusselt numbers for laminar flow at level 1 ad 2 of the dendritic branching-channel heat exchanger by the Reynolds number under the operating conditions of parallel flow closed circuit was calculated. Change of

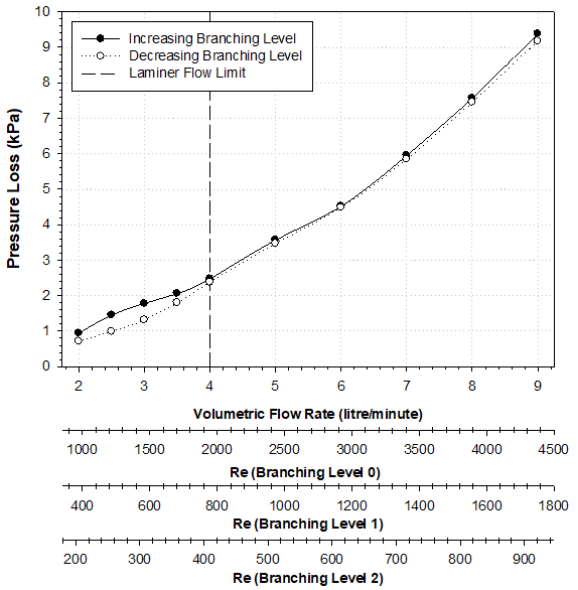

Figure 16. Change of the pressure losses towards increasing and decreasing branching levels by the volumetric flow rate and the Reynold number in the branches

the Nusselt number and the Reynolds numbers at level 0 is not shown in the diagram because the flow becomes turbulent flow for the values over 4.0 l/min.

In Fig. 22, Change of the Nusselt numbers calculated for the heating and cooling units at a maximum heating water inlet temperature of 65°C under the operating conditions of the counter-flow closed circuit by the Reynolds number is given. As it is seen in all of the three diagrams, the Nusselt numbers increased as the Reynold number increased.

Change of Total Heat Transfer Coefficient (U)

In the dendritic branching-channel heat exchanger, flow in each channel thermally and hydrodynamically redevelops at each branching level, and the boundary layer forms again for each level. Channel lengths being too short which do not allow the flow to fully develop thermally and hydrodynamically, and this causes an increase in h heat convection coefficient thus causing an increase in the total heat transfer coefficient.

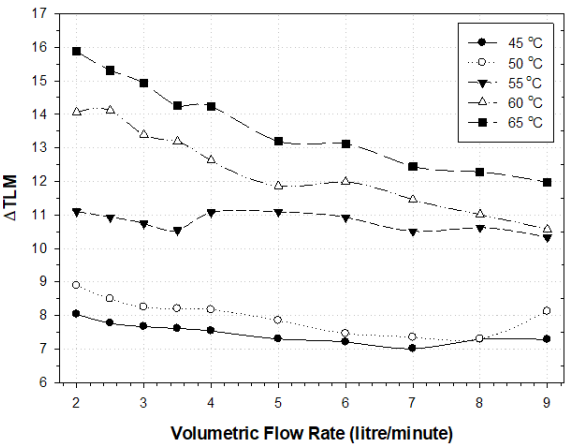

Figure 17. Change of the log mean temperature difference by the volumetric flow rate between the heating and cooling units in the parallel flow closed circuit

In Fig. 23-26, change of the total heat transfer coefficient U ($W/m^2.K$) by the volumetric flow rate $(\dot{V})$ for the parallel flow and counterflow operating conditions in open and closed circuits. It is seen in the diagrams given for the parallel flow and counterflow operations in the closed circuit that as the volumetric flow rate increases, the total heat transfer coefficient increases as well. Geometry of the dendritic branching-channel heat exchanger, increasing plate section towards increasing branching level, further occur-

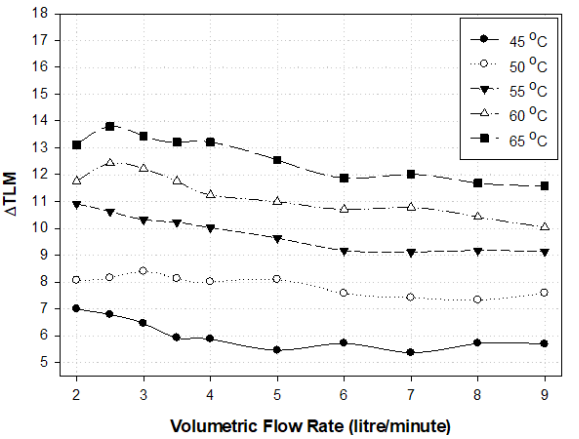

Figure 18. Change of the log mean temperature difference by the volumetric flow rate between the heating and cooling sides in the counterflow closed circuit

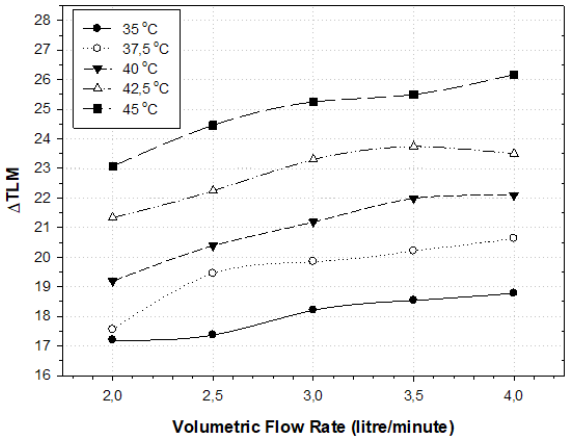

Figure 19. Change of the log mean temperature difference by the volumetric flow rate in the parallel flow closed circuit

rence of swirling flows, and also occurrence of jet flow at both points under the parallel flow conditions at the point where the distribution reservoirs are located cause the heat transfer coefficient to be found higher in case of parallel flow.

It is seen in the diagrams that the total heat transfer coefficient takes similar values depending on the temperature at a heating water inlet temperature of 45°C and a volumetric flow rate ranging between 2.0-4.0 l/min under the same operating conditions of the open circuit and closed circuit during the tests. Likewise, it is seen as a result of the tests that the most effective variable for change of the total heat transfer coefficient is the volumetric flow rate and the

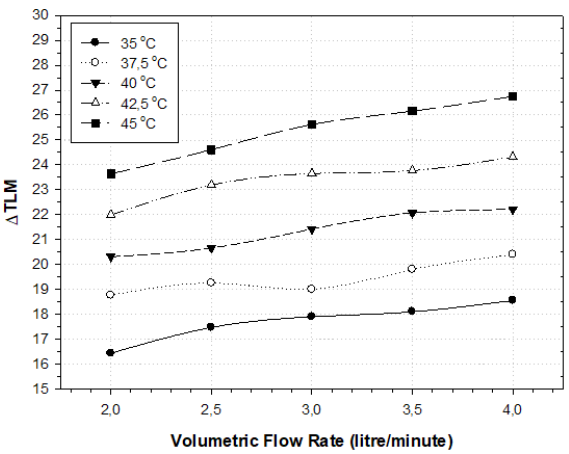

Figure 20. Change of the log mean temperature difference by the volumetric flow rate in the counter-flow open circuit

temperature range does not have a significant impact. It is a known fact that changing the inlet temperature of the heating unit of the heat exchanger would cause a change in the physical characteristics of the heating fluid. However, as a result of the test data it is not as effective as the volumetric flow rate value. It can be said according to the following four

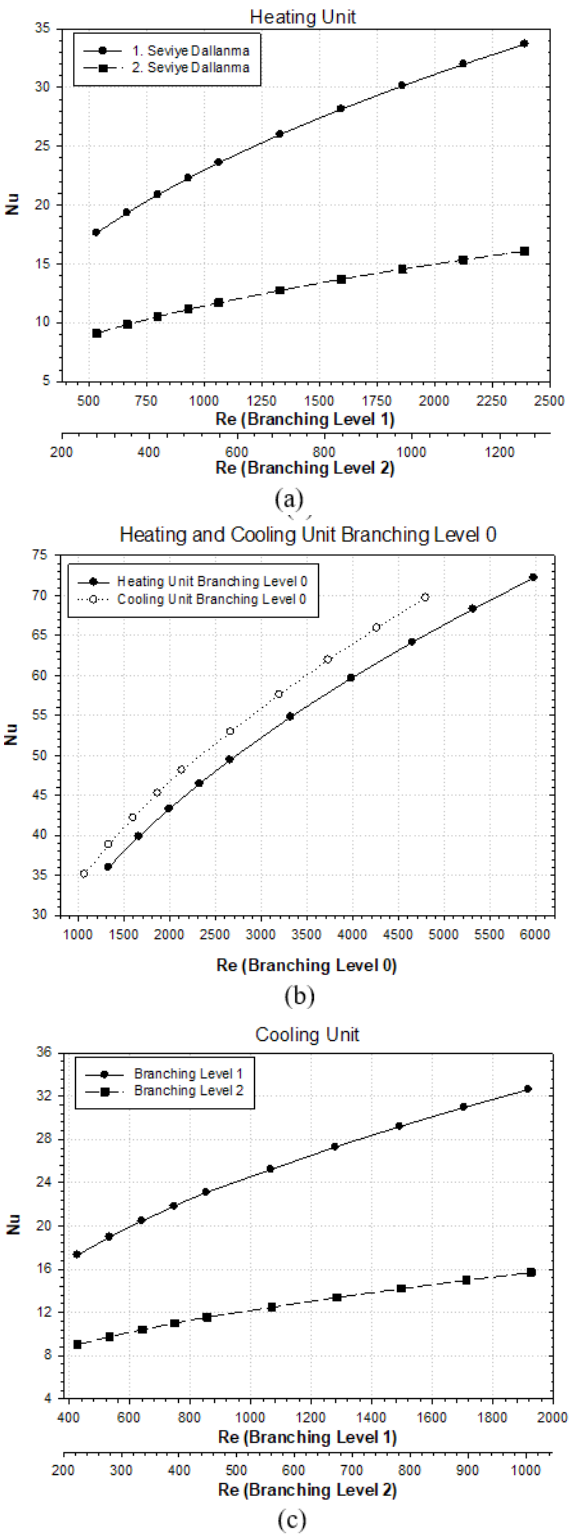

Figure 21. Change of the Nu-Re numbers at an inlet temperature of 65°C for the operating conditions of the parallel flow closed circuit

diagrams that the highest total heat transfer coefficient at the same temperature and flow rates ranging between 2.0-4.0 l/min for parallel flow and counterflow in cases of the closed and open circuits is seen in the parallel flow closed

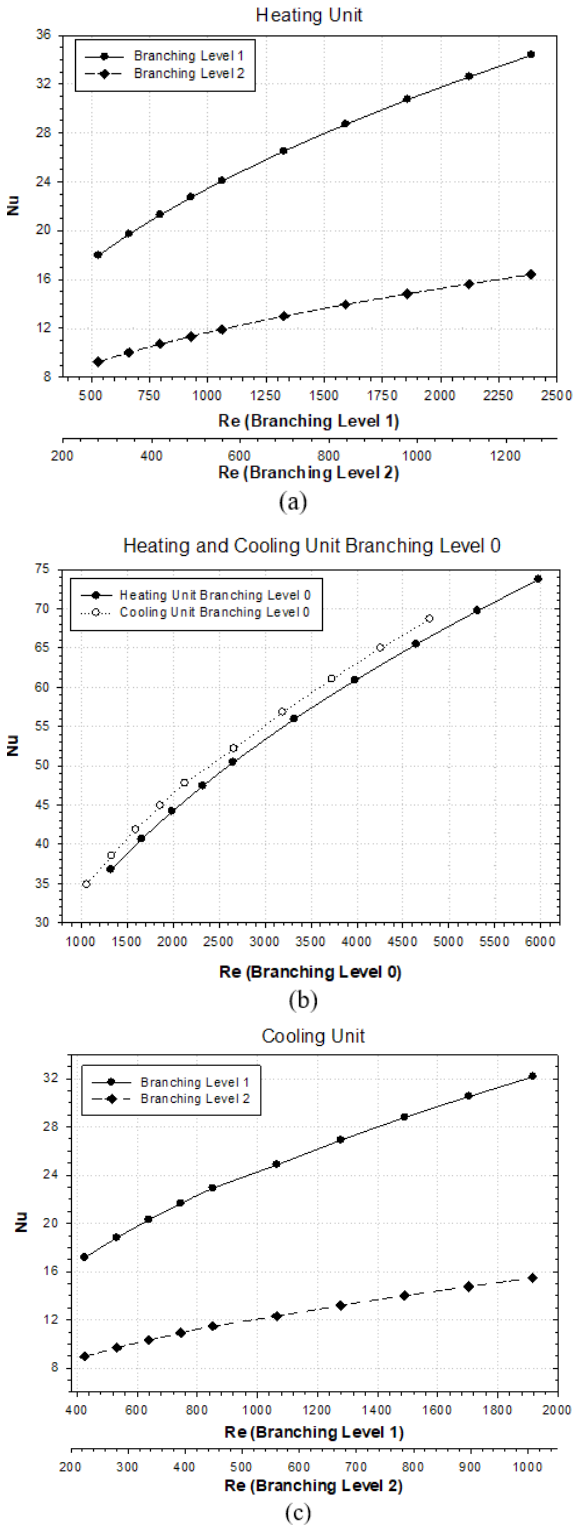

Figure 22. Change of the Nu-Re numbers at an inlet temperature of 65°C for the operating conditions of the counterflow closed circuit

circuit. It was observed that the total heat transfer coefficient U ($W/m^2.K$) showed a greater change in the parallel flow operation when compared to the counterflow operation at the same temperature and in the same range of flow rate for closed and open circuits.

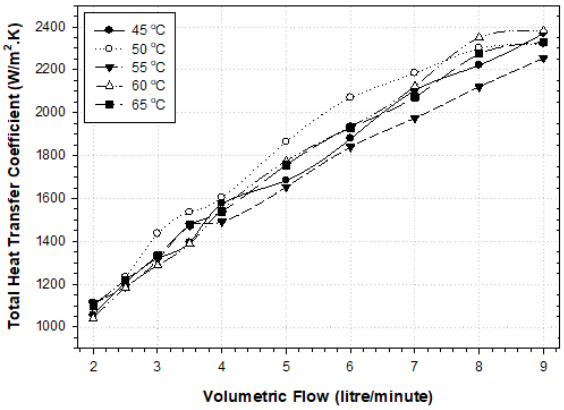

Figure 23. Change of the total heat transfer coefficient by the volumetric flow rate in the parallel flow closed circuit

Impact Analysis of Thermal Capacity Rates

In order to evaluate theoreticaland experimental researach and compare the impacts of thermal capacity rates on effectiveness, tests were carried out for the thermal capacity rates of *Cr*=1, *Cr*=0.25 and *Cr*=0.125 and a fluid inlet temperature of 65°C in the heating unit.

For a thermal capacity rate of Cr=1, fluid flow rates of the heating and cooling fluids are equal while entering into the system.

For a thermal capacity value of *Cr*=0.25, while the heating fluid ranges between 4.00 l/min – 8.00 l/min, the cooling fluid ranges between 1.00 l/min – 2.00 l/min. For a thermal capacity value of *Cr*=0.125, the heating fluid has a value of 8.00 l/min and the cooling fluid has a value of 1.00 l/min. Increasing the heating fluid inlet flow rate causes an increase in the mean temperature of the heated part of the middle plate and a further heat transfer to the fluid in the

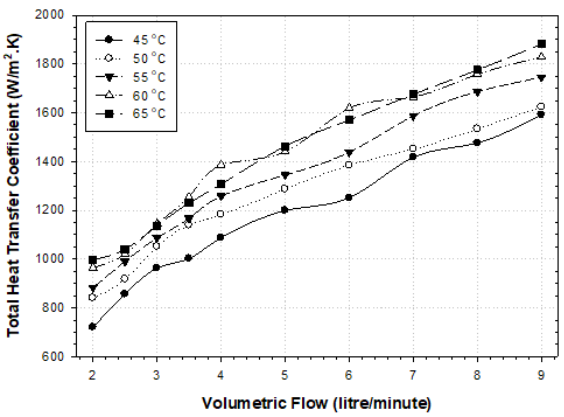

Figure 24. Change of the total heat transfer coefficient by the volumetric flow rate in the counterflow closed circuit

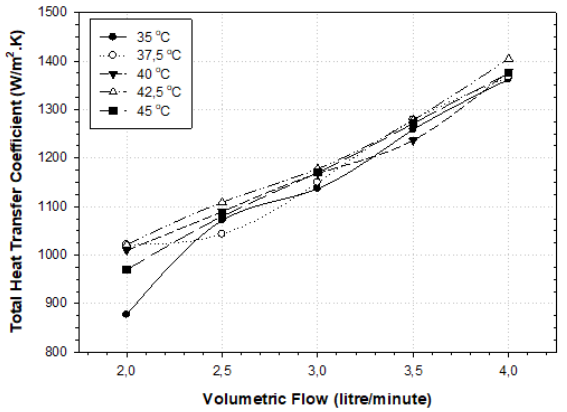

Figure 25. Change of the total heat transfer coefficient by the volumetric flow rate in the parallel flow open circuit

cooling side. In Fig. 27, results of the test, which shows the impacts of thermal capacity rates on effectiveness, are presented. As it is seen in the diagram, according to the ε-*NTU* method for different *Cr* values, it ranges between ε=0.24-0.58, *NTU*=0.3-0.81. In addition, a theoretical and experimental comparison was made according to the ε-*NTU* method for different *Cr* values, and it was seen that both experimental and theoretical results are consistent with the literature. As a result of the conducted tests, it was concluded that increasing the thermal capacity rates causes an increase in effectiveness (ε).

ANSYS-FLUENT ANALYSES

In this study, the designed dendritic branching-channel heat exchanger was geometrically modelled in Solid Works and numerically analyzed in ANSYS-Fluent 16.0 software package. While laminar model was applied in the tests up to a fluid flow rate of 4.0 l/min, k-ε turbulence model was applied in a higher flow rate than 4.0 l/min; and they were thermally analysed by solving the energy and Navier-Stokes equations. Upon the designed dendritic branching-channel heat exchanger;

i) Impacts of Temperature Change,
ii) Impacts of Flow Rate Change,
iii) Impacts of Operation Regime Change were examined in ANSYS-FLUENT.

It was seen that results obtained from the analyses performed by using ANSYS-FLUENT software was consistent with the test results. It was seen in the performed analyses that, in accordance with the constructal theory, flow rate of the fluid in sub-branches other than branching level zero (k=0) was lower when compared to the pipes which are coaxial with branching level zero. It was observed that this situation caused a lower flow rate in sub-branches from branching level one (k=1) and also further decrease of the rate since branching level two (k=2) was affected by branching level one.

CONCLUSION

In dendritic branching-channel heat exchangers, it is possible to achieve higher Nusselt numbers and to increase the heat transfer rate by carefully calculating channel sections, channel geometries and channel dimensions. Hydrodynamical and thermal re-development of the Nusselt number and heat transfer value in each channel and at each branching level is an important characteristic of this geometry. In Fig. 11-14, change of the heat transfer for parallel flow and counter-flow in the open and closed circuits by the volumetric flow rate was given, and it was observed that the heat transfer value increased with increasing volumetric flow rate.

In Fig. 15, change of the ratio of the heat transfer value to the inflowing heat by the volumetric flow rate is given, and since the mean temperature of the test zone in the experiment system was lower in the open circuit, it was determined that this ratio was higher in the open circuit.

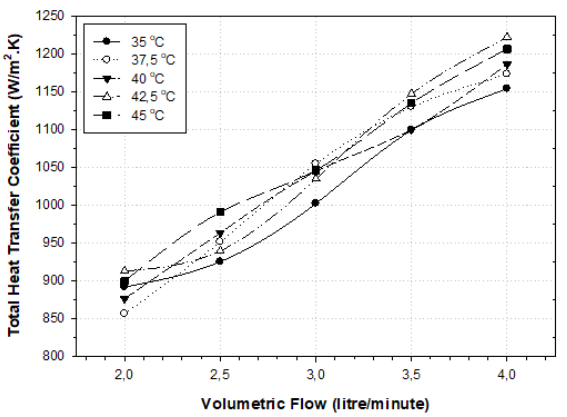

Figure 26. Change of the total heat transfer coefficient by the volumetric flow rate in the counterflow open circuit

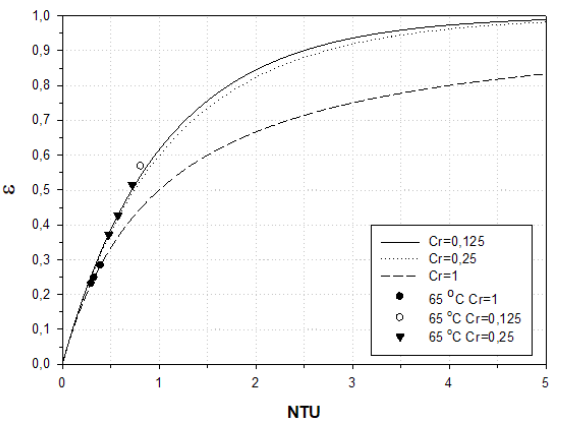

Figure 27. Impacts of the thermal capacity rates on effectiveness

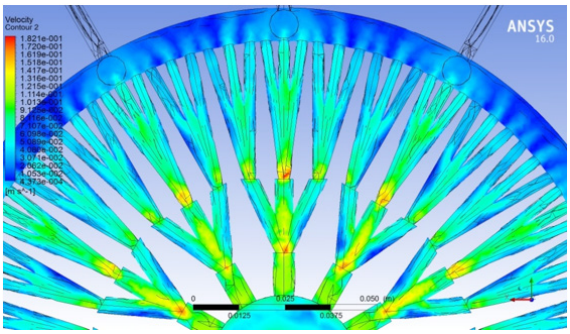

Figure 28. Rate distributions in the heat exchanger for 2.0 l/min for the flow towards increasing branching levels

In Fig. 16, change of the pressure losses towards increasing and decreasing branching levels by the volumetric flow rate and the Reynolds numbers in the branches is presented, and it is seen that pressure losses increase with increasing volumetric flow rates and Reynolds numbers in the branches. This result indicates that an increase in branching level is not important in the flow channels with such dendritic branching (fractal) channel structure.

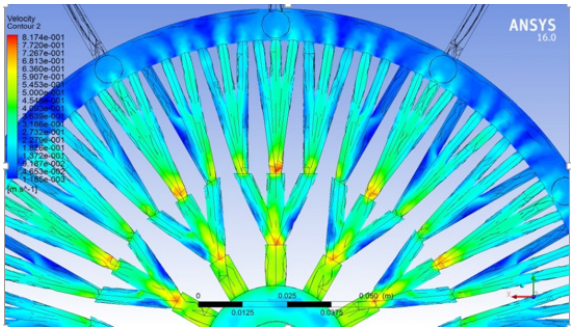

Figure 29. Rate distributions in the heat exchanger for 9.0 l/min for the flow towards increasing branching levels

In the diagrams in Fig. 17-20, change of the log mean temperature difference by the volumetric flow rate for parallel flow and counter-flow operation in open and closed circuits is given. In case of the closed circuit, the log mean temperature difference gradually decreases in both flow regimes as the volumetric flow rate increases. In case of the open circuit, the log mean temperature difference gradually increases in both flow regimes as the volumetric flow rate increases. The logmean temperature difference increases with increasing inlet temperature.

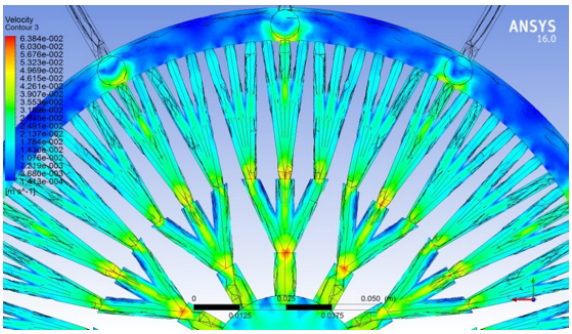

Figure 30. Rate distributions in the heat exchanger for 2.0 l/min for the flow towards decreasing branching levels

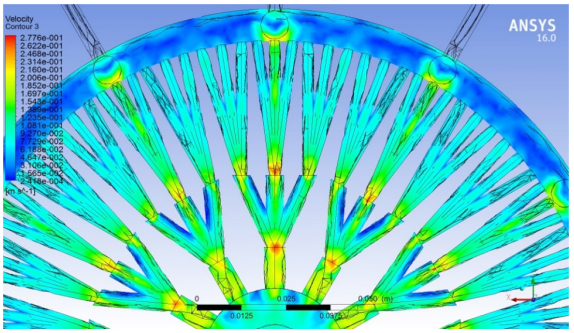

Figure 31. Rate distributions in the heat exchanger for 9.0 l/min for the flow towards decreasing branching levels

In the diagrams in Fig. 21-22, changes of Nu-Re numbers for different inlet temperatures in the heating side under parallel flow and counterflow operating conditions in closed and open circuits at different levels. As it is seen in the diagrams, Nusselt numbers increase with increasing Reynolds numbers, depending on branching levels at varying flow rates and temperatures. Likewise, it is graphically showed that a greater increase is seen in the Nusselt number at branching level one. The volumetric flow rate increasing in the heating and cooling sides caused the Nusselt number to increase in a decelerating manner; and thus, it caused the heat convection coefficient, and therefore the heat transfer

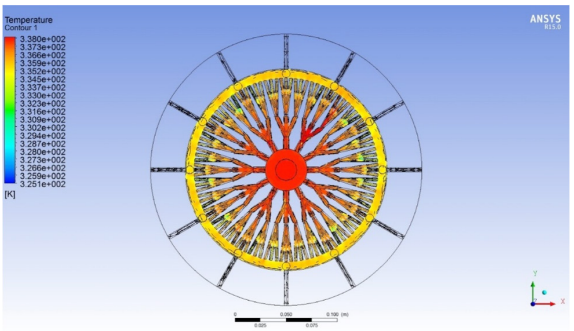

Figure 32. Temperature distribution in the heating unit under the parallel flow closed circuit conditions for a heating fluid inlet temperature of 65°C and a flow rate of 9.0 l/min

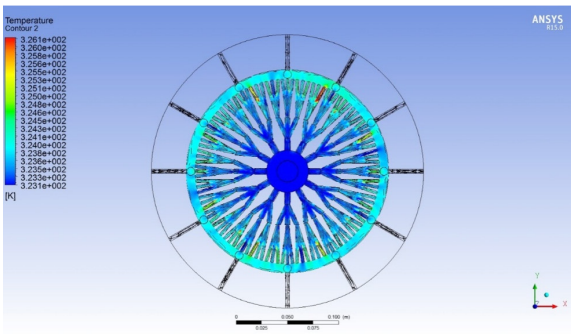

Figure 33. Temperature distribution in the cooling unit under the parallel flow closed circuit conditions for a heating fluid inlet temperature of 65°C and a flow rate of 9.0 l/min

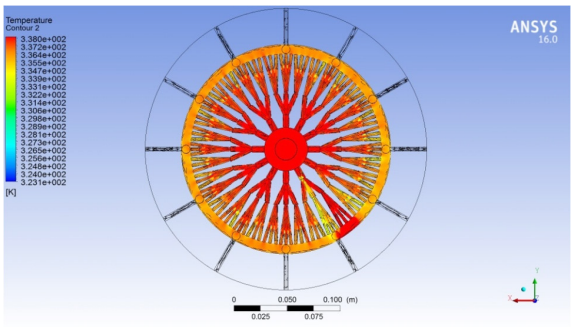

Figure 34. Temperature distribution in the heating unit under the counterflow closed circuit operating conditions for a heating fluid inlet temperature of 65°C and a flow rate of 9.0 l/min

value Q(Watt), to increase in a decelerating manner with the volumetric flow rate.

Change of the total heat transfer coefficient (U) by the volumetric ($\dot{V}$) flow rate according to the tests performed for parallel flow and counterflow under the closed circuit operating conditions (45, 50, 55, 60 and 65°C) are given in Figure 23-26 and under the open circuit operating conditions (35, 37.5, 40, 42.5 and 45°C) are given in Figure 33-34. It is seen in the diagrams of the experimental results that the total heat transfer coefficient increased by increasing volumetric flow rate under both parallel flow and counterflow conditions. In case of the parallel flow closed circuit, the total heat transfer coefficient was higher when compared to the counterflow. The same can be said for the open circuit as well.

Since the tests were carried out under *Cr*=1 conditions of the dendritic branching-channel heat exchanger, volumetric flow rates for the fluids circulating in both units are equal. At a thermal capacity flow rate of *Cr*=1, it was seen that the maximum effectiveness coefficient value is at ε=0.30 level. When the thermal capacity flow rates were changed to *Cr*=0.125 level, it was seen that ε=0.58 and *NTU*=0.81 in case of counterflow operation. In the diagram in Figure 27, the increased inlet flow rate of the heating fluid increased the mean temperature on the plate and this caused the effectiveness coefficient to rise.

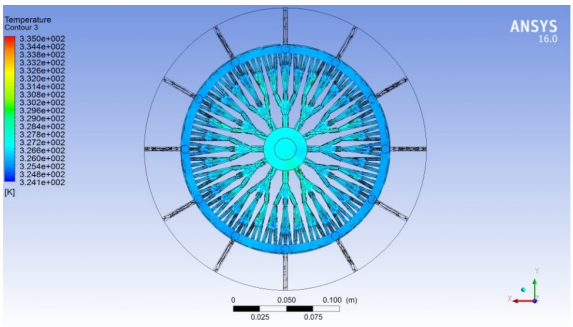

Figure 35. Temperature distribution in the cooling unit under the counter-flow closed circuit operating conditions for a heating fluid inlet temperature of 65°C and a flow rate of 9.0 l/min

Changes of rate and temperature were analyzed for different flow rate and temperature values in ANSYS, and the results are given as diagrams in Fig. 31-35.

Symbols

A Heat Transfer Surface Area (m^2)

A_0 Level 0 Branching Heat Transfer Surface Area

A_1 Level 1 Branching Heat Transfer Surface Area

A_2 Level 2 Branching Heat Transfer Surface Area

A_k Level k Channel Surface Area

C_h Thermal Capacity Flow Rate of Hot Fluid (W/K)

C_c Thermal Capacity Flow Rate of Cold Fluid (W/K)

C_{max} Maximum Thermal Capacity Flow Rate (W/K)

C_{min} Minimum Thermal Capacity Flow Rate (W/K)

C_r Ratio of Thermal Capacity Flow Rates

D Pipe Diameter (m)

$D_{h,k}$ Level k Branch Hydraulic Diameter (m)

D_h Hydraulic Diameter (m)

ΔP Pressure Difference (Pa)

ΔT Temperature Difference (K)

ε Effectiveness

k Thermal Conductivity Coefficient (W/mK)

L_k Level k Branch Length (m)

L Length (m)

$LMTD$ Log Mean Temperature Difference (°C)

$\dot{m}$ Volumetric Flow Rate (kg/s)

$\dot{m}_h$ Hot Fluid Flow Rate (kg/s)

$\dot{m}_c$ Cold Fluid Flow Rate (kg/s)

$MEMS$ Micro Electromechanical Systems

N_k Number of Channels

N Number of Branches

Nu Nusselt Number

NTU Number of Transfer Units

ρ Density

Q From Hot Fluid to Cold Fluid Heat Transfer Value (W)

$Q_{\%thermal\ difference}$ % difference between the Heat Entering into the Experiment System and the Heat Received from the System

Q_r Heat Received from the Experiment System (W)

Q_g Heat Entering into the Experiment System (W)

Q_{losses} Heat Loss (W)

Q_{max} Maximum Possible Heat Transfer from Hot Fluid to Cold Fluid (W/)

Q_{mean} Mean of the Heat Entering into the Experiment System and the Heat Received from the System

$Q_{con.}$ Heat Transferred through Convection (W)

Q_{top} Total of Convection, Radiation and Lost Heat Values (W)

$Q_{rad.}$ Heat Transferred through Radiation (W)

Re Reynolds Number

T Temperature (°C)

$T_{h,i}$ Inlet Temperature of the Hot Fluid Entering into the Heat Exchanger (K)

$T_{h,o}$ Outlet Temperature of the Hot Fluid Coming out of the Heat Exchanger (K)

$T_{c,i}$ Inlet Temperature of the Cold Fluid Entering into the Heat Exchanger (K)

$T_{c,o}$ Outlet Temperature of the Cold Fluid Coming out of the Heat Exchanger (K)

U Total Heat Transfer Coefficient (W/m2.K)

μ Dynamic Viscosity (Pa.s)

ν Viscosity

V Velocity (m/s)

References

1. Andhare RS, Shooshtari A, Dessiatoun SV, Ohadi MM. Heat transfer and pressure drop characteristics of a flat plate manifold microchannel heat exchanger in counter flow configuration. Applied Thermal Engineering 96 (2016) 178-189.
2. Bejan A. Constructal-theory network of conducting paths for cooling a heat generating volume. International Journal of Heat and Mass Transfer 40 (1997) 799-816.
3. Bejan A. Dendritic constructal heat exchanger with small-scale crossflows and larger-scales counterflows. International Journal of Heat and Mass Transfer 45 (2002) 4607-4620.
4. Bonjour J, Rocha LAO, Bejan A, Meunier F. Dendritic fins optimization for a coaxial two-stream heat exchanger. International Journal of Heat and Mass Transfer 47 (2003) 111-124.
5. Calamas D, Baker J. Tree-like branching fins: Performance and natural convective heat transfer behavior. International Journal of Heat and Mass Transfer 62 (2013) 350-361.
6. Chen Y, Cheng P. An experimental investigation on the thermal efficiency of fractal tree-like microchannel nets. International Communications in Heat and Mass Transfer 32 (2005) 931-938.
7. Chen Y, Zhang C, Shi M, Yang Y. Thermal and Hydrodynamic Characteristics of Constructal Tree-Shaped Minichannel Heat Sink. American Institute of Chemical Engineers 56 (2010) 2018-2029.
8. Da Silva AK, Lorente S, Bejan A. Constructal multi-scale tree-shaped heat exchangers. Journal Of Applied Physics 96 (2004) 1709-1718.
9. Daniels BJ, Pence DV, Liburdy JA. Predictions of Flow Boiling in Fractal-like Branching Microchannels. ASME Proceedings of IMECE 2005, Orlando, Florida, USA, 5 – 11 November, pp. 359-368, 2005.
10. Escher W, Michel B, Poulikakos D. Efficiency of optimized bifurcating tree-like and parallel microchannel networks in the cooling of electronics. International Journal of Heat and Mass Transfer 52 (2009) 1421–1430.
11. Ghodoossi L. Thermal and hydrodynamic analysis of a fractal microchannel network. Energy Conversion and Management 46 (2005) 771-788.
12. Hernando NG, Iborra AA, Rivas UR, Izquierdo M. Experimental investigation of fluid flow and heat transfer in a single-phase liquid flow micro-heat exchanger. International Journal of Heat and Mass Transfer 52 (2009) 5433-5446.
13. Heymann D, Pence D, Narayanan V. Optimization of fractal-like branching microchannel heat sinks for single-phase flows. International Journal of Thermal Sciences 49 (2010) 1383-1393.
14. [14] Hong FJ, Cheng P, Ge H, Goh Teck Joo. Conjugate heat transfer in fractal-shaped microchannel network heat sink for integrated microelectronic cooling application. International Journal of Heat and Mass Transfer 50 (2007) 4986-4998.
15. Hung TC, Yan WM, Li WP. Analysis of heat transfer characteristics of double-layered microchannel heat sink. International Journal of Heat and Mass Transfer 55 (2012) 3090-3099.
16. Kim DK. Thermal optimization of branched-fin heat sinks subject to a parallel flow. International Journal of Heat and Mass Transfer 77 (2014) 278–287.
17. Kwak Y, Pence D, Liburdy J, Narayanan V. Gas-liquid flows in a microscale fractal-like branching flow network. International Journal of Heat and Fluid Flow 30 (2009) 868-876.
18. Lee YJ, Singh PK, Lee PS. Fluid flow and heat transfer investigations on enhanced microchannel heat sink using oblique fins with parametric study. International Journal of Heat and Mass Transfer 81 (2015) 325–336.

19. Lin WW, Lee DJ. Diffusion-convection process in a branching fin. Chemical Engineering Communications 158 (1997) 59-70.
20. Meyer JP, Van der Vyver H. Heat Transfer Characteristics of a Quadratic Koch Island Fractal Heat Exchanger. Heat Transfer Engineering 26 (2005) 22-29.
21. Moreno A, Murphy K, Wilhite BA. Parametric study of solid-phase axial heat conduction in thermally integrated microchannel networks. Industrial Engineering Chemistry Research 47 (2008) 9040-9054.
22. Murray CD. The physiological principle of minimum work; I. The vascular system and the cost of blood volume. P.N.A.S. 12 (1926) 207–214.
23. Park KT, Kim HJ, Kim DK. Experimental study of natural convection from vertical cylinders with branched fins. Experimental Thermal and Fluid Science 54 (2014) 29-37.
24. Pence DV. Reduced Pumping Power and Wall Temperature in Microchannel Heat Sinks with Fractal-like Branching Channel Networks. Microscale Thermophysical Engineering 6 (2002) 319-330.
25. Pence D, Enfield K. Inherent Benefits in Microscale Fractal-like Devices for Enhanced Transport Phenomena. Design and Nature II Comparing Design in Nature with Science and Engineering, WIT Press (2004) 317-327.
26. Pence DV. Improved Thermal Efficiency and Temperature Uniformity using Fractal-like Branching Channel Networks. Proceedings of the International Conference on Heat Transfer and Transport Phenomena in Microscale, ed. G.P. Celata, Begell House, New York, pp. 142-148, 2000.
27. Xu P, Yu B, Yun M, Zou M. Heat conduction in fractal tree-like branched networks. International Journal of Heat and Mass Transfer 49 (2006) 3746–3751.
28. Peterson RB. Numerical modeling of conduction effects in microscale counterflow heat exchangers. Microscale Thermophysical Engineering 3 (1999) 17-30.
29. Salakij S, Liburdy JA, Pence DV, Apreotesi M. Modeling in situ vapor extraction during convective boiling in fractal-like branching microchannel networks. International Journal of Heat and Mass Transfer 60 (2013) 700-712.
30. Da Silva AK, Bejan A. Dendritic counterflow heat exchanger experiments. International Journal of Thermal Sciences 45 (2006) 860-869.
31. [31] Stief T, Langer OU, Schubert K. Numerical investigations of optimal heat conductivity in micro heat exchangers. Chemical Engineering Technology 21 (1999) 297– 303.
32. Tuckerman DB, Pease RFW. High-performance heat sinking for VLSI. IEEE Electron Device Letters 2 (1981) 126-129.
33. Vafai K, Zhu L. Analysis of two-layered microchannel heat sink concept in electronic cooling. International Journal of Heat and Mass Transfer 42 (1999) 2287–2297.
34. Wechsatol W, Lorente S, Bejan A. Optimal tree-shaped networks for fluid flow in a disc-shaped body. International Journal of Heat and Mass Transfer 45 (2002) 4911–4924.
35. West GB, Brown JH, Enquist BJ. A General Model for the Origin of Allometric Scaling Laws in Biology. Science 276 (1997) 122-126.
36. Xia C, Fu J, Lai J, Yao X, Chen Z. Conjugate heat transfer in fractal tree-like channels network heat sink for high-speed motorized spindle cooling. Applied Thermal Engineering 90 (2015) 1032-1042.
37. Xu S, Wang W, Fang K, Wong CN. Heat transfer performance of a fractal silicon microchannel heat sink subjected to pulsation flow. International Journal of Heat and Mass Transfer 81 (2015) 33-40.
38. Yang Y, Morini GL, Brandner JJ. Experimental analysis of the influence of wall axial conduction on gas-to-gas micro heat exchanger effectiveness. International Journal of Heat and Mass Transfer 69 (2014) 17-25.
39. Zhang C, Lian Y, Yu X, Liu W, Teng J, Xu T, Hsu CH, Chang YJ, Greif R, Numerical and experimental studies on laminar hydrodynamic and thermal characteristics in fractal-like microchannel networks. Part B: Investigations on the performances of pressure drop and heat transfer. International Journal of Heat and Mass Transfer 66 (2013) 939-947.
40. Zimparov VD, Da Silva AK, Bejan A. Constructal tree-shaped parallel flow heat exchangers. International Journal of Heat and Mass Transfer 49 (2006) 4558-4566.
41. Chong SH, Ooi KT, Wong TN. Optimisation of single and double layer counter flow microchannel heat sinks. Applied Thermal Engineering 22 (2002) 1569–1585.
42. Lee YJ, Singh PK, Lee PS. Fluid flow and heat transfer investigations on enhanced microchannel heat sink using oblique fins with parametric study. International Journal of Heat and Mass Transfer 81 (2015) 325–336.
43. Bier W, Keller W, Linder G, Seidel D, Schubert K, Martin H. Gas to gas heat transfer in micro heat exchangers. Chemical Engineering and Processing: Process Intensification 32 (1993) 33–43.
44. Bejan A. Street network theory of organization in nature. Journal of Advanced Transportation, 30 (1996), 85–107.
45. Bejan A. Constructal theory of pattern formation, Hydrology and Earth System Sciences 11 (2007) 753–768.
46. Bonjour J. Rocha LAO, Bejan A, Meunier F. Dendritic fins optimization for a coaxial two-stream heat exchanger. International Journal of Heat and Mass Transfer 47 (2003) 111–124.
47. Cohn DL. Optimal systems: I. The vascular system. Bulletin Of MathematicalBiophysics 16 (1954) 59–74.
48. Lee DJ, Lin WW. Second law analysis on fractal-like fin under crossflow. American Institute of Chemical Engineers Journal 41(1995) 2314–2317.
49. Lin WW, Lee DJ. Diffusion–convection process in a branching fin, Chemical Engineering Communications 158 (1997) 59–70.
50. Chen Y, Cheng P. Heat transfer and pressure drop in fractal tree-like microchannel nets. International Journal of Heat and Mass Transfer 45 (2002) 2643–2648.
51. Park KT, Kim HJ, Kim DK. Experimental study of natural convection from vertical cylinders with branched fins. Experimental Thermal and Fluid Science 54 (2014) 29–37.
52. Lorenzini G, Rocha LAO. Constructal design of Y-shaped assembly of fins. International Journal of Heat and Mass Transfer 49 (2006) 4552–4557
53. Cengel YA, Cimbala JM. Akiskanlar Mekanigi Temelleri ve Uygulamalari. Guven Bilimsel, İzmir, 2007.
54. Cengel YA. Isi ve Kutle Transferi. Guven Kitabevi, Izmir, 2011.
55. Genceli OF. Isı Degistiricileri. Birsen Yayınevi, İstanbul, 2010.
56. Stephan K, Preusser P. Heat Transfer and Critical Heat Flux in Pool Boiling of Binary and Ternary Mixtures. German Chemical Engineering, 2 (1979) 161-169.